

## Uncertainty in Fast Reactor-Relevant Critical Benchmark Simulations Due to Unresolved Resonance Structure

Jonathan A. Walsh<sup>1,\*</sup>, Benoit Forget<sup>2</sup>, Kord S. Smith<sup>2</sup>, Forrest B. Brown<sup>3</sup>

<sup>1</sup>Lawrence Livermore National Laboratory, 7000 East Avenue, Livermore, CA, USA 94550

<sup>2</sup>Massachusetts Institute of Technology, 77 Massachusetts Avenue, 24-107, Cambridge, MA, USA 02139

<sup>3</sup>Los Alamos National Laboratory, P.O. Box 1663, Los Alamos, NM, USA 87545

\*walsh@llnl.gov

**Abstract** - A capability to generate a single realization of resonance parameters in the unresolved resonance region for use throughout a single neutron transport simulation and its applications to nuclear data benchmarking are presented. This approach differs from the typical probability table treatment in which, effectively, a new realization of resonance structure is sampled at each cross section calculation event. The capability is implemented in a continuous-energy Monte Carlo code and used to demonstrate the calculation of expected value tallies which more rigorously account for the effects of unresolved resonance structure. The expected values computed by averaging results of independent simulations, each using a single, distinct realization of resonance structure, are observed to be in good agreement with results obtained by using a new realization of resonance parameters for each cross section calculation. However, the range of results computed with each of several realizations of resonance structure can be several times larger than that which is expected as a result of statistical uncertainty. That is, uncertainty in the precise, energy-dependent resonance structure of cross sections in the unresolved region induces an additional, intrinsic uncertainty that cannot be reduced by simulating a greater number of neutron histories. In simulations of an intermediate/fast spectrum system, the 95% confidence interval of  $k_{\infty}$  eigenvalues computed with different realizations of resonance structure is  $\sim 300$  pcm greater than the purely statistical interval which is ordinarily reported.

## I. INTRODUCTION

Nuclides with structured neutron cross sections that have not yet been resolved in energy to the precision of individual resonances are said to have an unresolved resonance region (URR). This situation may arise due to insufficient experimental precision in cross section measurements or, more generally, as a result of a lack of experimental data on which to perform a resolved resonance evaluation. In such cases, neither the resonance parameters (i.e., resonance energies and partial reaction widths) nor pointwise data representations of individual resonances are available in the URR. Cross sections must instead be described by average resonance parameters and the theoretical distributions of those parameters [1].

This is a fundamentally different type of uncertainty than is usually discussed when dealing with resolved resonances. To be sure, there are uncertainties in resolved resonance data which can impact simulation results. However, the uncertainties on resolved resonance parameters propagate to uncertainties on *cross section* values, not the underlying resonance structure. Thought of another way, resolved resonance parameters are deterministic and result in energy-dependent cross section values with some uncertainty — typically no more than a few percent for the principal reactions of the nuclides which are most relevant to nuclear science and technology applications. Contrast this with the stochastic nature of the URR in which the energy and partial widths of any single resonance are entirely unknown and must be randomly sampled from theoretical distributions.

To mitigate the problem of unknown URR resonance structure, the probability table method was developed [2]. This method relies on the pre-generation of discrete cross section magnitudes and associated probabilities at discrete energies and temperatures. These discrete data are then sampled within Monte Carlo transport simulations according to their probabilities. Probability tables provide a better model of resonance structure — and the resulting self-shielding effects — than average cross sections because, at a given energy and temperature, a range of cross section magnitudes may be sampled. More recently, an approach by which a new realization of resonance parameters is sampled on-the-fly and cross sections are calculated directly *at each event* in the simulation was introduced [3]. This direct, on-the-fly scheme represents a generalization of the probability table method in that it treats the energy, temperature, and cross section magnitude variables continuously, rather than in a discrete fashion.

A natural alternative to probabilistic re-generation of URR resonance structure within a simulation is to generate a single realization of resonance parameters at the start of a simulation and use that same, unchanging realization throughout. Such a realization is still probabilistic in the sense that it is generated by sampling resonance parameters from distributions, but once sampled, a single set of resonance parameters is valid in all cross section calculations, for all neutron histories, as is the case in nature. Similar solutions were briefly explored for modeling the resonance structure of URR cross sections prior to the advent, and subsequent widespread adoption, of the probability table method [4, 5]. However, the methods employed to actually generate resonance realizations often made very crude approximations [5, 6]. Use of the resulting

fine structure cross sections in Monte Carlo calculations was generally intractable from a computational perspective. Due to the great expense of both generating resonance realizations and utilizing the continuous-energy cross section values from those realizations in any meaningful calculation, these alternate methods were largely abandoned in favor of probability table treatments.

With an independent realization treatment, there is a further question: how does one know that the single realization generated accurately represents the true resonance structure which exists in nature? The answer, of course, is that one cannot ever make that determination. In fact, the sampled resonance structure will invariably be a poor representation of nature, at least with respect to cross section values at specific energies. Though a sampled ensemble of resonances will constitute a viable realization of nature because it is reconstructed from a set of resonance parameters that is drawn from a distribution of physically allowable values, no single realization can be trusted more or less than any other realization to represent the single, true cross section resonance structure which exists in nature. It would take an infinite number of realizations to stumble upon the correct ensemble, and one could not even recognize it if he did because the resonance parameters which describe the actual URR resonances are, by definition, unknown. For this reason, some efforts were aimed at developing methods for generating a *recommended* realization [7] and also quantifying integral calculation uncertainties that arise from a lack of knowledge of the true URR resonance structure [4, 8]. These efforts, too, were largely abandoned with the adoption of the probability table method.

Motivated by the notion that a single, persistent URR realization is, in many ways, a better model of nature and enabled by modern computational resources, it is appropriate to revisit single URR resonance structure realizations for use in Monte Carlo simulations. This work explores the implications of the root cause of the URR phenomenon, which is to say a lack of knowledge of *precise resonance structure*, as they relate to uncertainties in critical benchmark simulation results.

The ability to compute more rigorous expected values via independent URR realizations and the loss of that ability when using probability tables are discussed further in Section II. The implementation of the capability to generate independent resonance ensembles and utilize them within a transport simulation are outlined in Section III. Results of simulations performed with a continuous-energy Monte Carlo neutron transport code which demonstrate the calculation of expected values and corresponding uncertainties are presented in Section IV. A summarizing discussion is found in Section V.

## II. INDEPENDENT REALIZATIONS VS. PROBABILITY TABLES

One shortcoming present in both the probability table and direct methods is the generation of what is effectively a new

realization of resonances at each event. Both methods assume that neutrons, at a given energy, experience resonance structure that is independent of all structure previously encountered. The direct approach explicitly generates a new realization while the probability table method does so implicitly by sampling cross section magnitudes which represent different realizations. Both of these models are unphysical and result in an artificial averaging over all possible resonance structures whereas, in nature, a single resonance structure exists.

A solution to the above dilemma is to generate independent realizations of URR resonance structure and utilize each of these realizations throughout its own independent Monte Carlo transport simulation. By doing so, expected value tallies which are more rigorous than those obtained from simulations relying on probability tables are accessible. The value obtained by taking the mean of the tally results of  $N$  independent simulations, each using cross sections from one of  $N$  independent URR resonance structure realizations throughout, gives the expected value for the tally. This is in contrast to taking the mean of the tally results of  $N$  independent simulations, each using probability tables, which gives a value that is based on  $N$  simulations which each utilize cross sections representing several different realizations of resonance structure at once. As a consequence, it is not guaranteed that simulations using probability tables or direct calculations must reproduce true expected value tallies. In general, the re-generation of a new resonance structure at each event will introduce a bias in calculated results. This difference between results computed with probability tables and those computed by averaging independent simulations can be illustrated with a simple example:

If there is a point-source at  $E_0$ ,

$$S(E) = S_0 \int_{-\infty}^{\infty} dE \delta(E - E_0), \quad (1)$$

and there are exactly two equiprobable resonance structures,

$$\begin{aligned} \Sigma_1(E_0 \rightarrow E_1) &= 0; \\ \Sigma_1(E_1 \rightarrow E_2) &= \infty; \\ \Sigma_1(E_2) &= 0 \end{aligned} \quad (2)$$

and

$$\begin{aligned} \Sigma_2(E_0 \rightarrow E_1) &= \infty; \\ \Sigma_2(E_1) &= 0; \\ \Sigma_2(E_2) &= 0, \end{aligned} \quad (3)$$

one concludes that two independent simulations, each utilizing a different one of the two possible realizations, yield an expectation of 0.5 interactions for each of the  $S_0$  source particles, whereas probability tables yield 0.75. The probabilities of the possible outcomes are summarized in Table I.

TABLE I. Probabilities

Method	Interactions		
	0	1	2
Probability tables	0.5	0.25	0.25
Independent realizations	0.5	0.5	0.0

Another advantage of independent realizations relative to probability tables is that if a nuclide’s cross sections are calculated at a specific energy, identical cross section values will be computed in subsequent calculations at that same energy (cf. [2, 3]). As a corollary, cross section values computed at energies which neighbor one another will reflect the correlated resonance structure between the two energies. That is, if cross section values are computed at a resonance energy once, all cross sections computed very close to that energy will have a similarly large magnitude. This can be important in fine-group spectrum calculations which require the same resonance structure to be experienced by all neutrons, at all events, in order to reveal the peaks and valleys in reaction rate tallies which occur across energy as a result of individual resonances.

In closing the discussion comparing the probability table method with independent realizations, it is worth noting that, in addition to the calculation of unbiased expected value tallies, independent URR realizations enable a more accurate calculation of those tallies’ uncertainties. It is actually a principal advantage of independent URR realizations, relative to probability tables, that because each simulation utilizing a new, independent realization represents a viable realization of nature, it is possible to determine an expected spread of tally results which accounts for the stochastic uncertainty typical of Monte Carlo simulations as well as the physical uncertainty stemming from a lack of knowledge of URR resonance structure. The results presented in Section IV demonstrate that the spread of tally results obtained from independent simulations using unchanging URR realizations — information that cannot be ascertained from simulations in which the probability table or direct methods are used — can be significant for intermediate/fast spectrum systems.

### III. GENERATING URR REALIZATIONS

The capability to generate single, nuclide-specific realizations of URR resonance parameters for continued use throughout a simulation is implemented in the continuous-energy Monte Carlo transport code OpenMC [9]. This implementation requires only straightforward modifications to the probability table generation and direct calculation algorithms. The mechanics of sampling level spacings and partial reaction widths are unchanged. At the initialization of a simulation, before any

neutron histories are run, starting from the resonance energy,  $E_\lambda$ , of the highest-energy resolved resonance region resonance with a given spin sequence (defined by orbital and total angular momentum quantum numbers,  $l$  and  $J$ , respectively), the Wigner distribution for level spacings [10],

$$P_W\left(\frac{D^{l,J}(E_\lambda)}{\langle D^{l,J}(E_\lambda) \rangle}\right) = \frac{\pi D^{l,J}(E_\lambda)}{2\langle D^{l,J}(E_\lambda) \rangle} \exp\left(-\frac{\pi D^{l,J}(E_\lambda)^2}{4\langle D^{l,J}(E_\lambda) \rangle^2}\right), \quad (4)$$

is sampled to determine the distance in energy,  $D^{l,J}$ , to the next resonance with that same spin sequence. Using this new resonance energy as a starting point, another level spacing is sampled to determine the placement of the next, and so on. For each resonance energy that is sampled, partial widths for reaction  $r$ ,  $\Gamma_r$ , are sampled from a  $\chi^2$  distribution [11],

$$P_{\chi^2(\mu_r)}(y) = \frac{\exp\left(-\frac{y}{2}\right)y^{\frac{\mu_r}{2}-1}}{2^{\mu_r/2}G\left(\frac{\mu_r}{2}\right)}; \quad (5)$$

$$y \equiv \mu_r \frac{\Gamma_r^{l,J}}{\langle \Gamma_r^{l,J}(E_\lambda) \rangle},$$

where  $\mu_r(l, J)$  is a reaction channel-dependent number of degrees of freedom and the  $G\left(\frac{\mu_r}{2}\right)$  term in (5) is the Gamma function,

$$G\left(\frac{\mu_r}{2}\right) = \int_0^\infty x^{\frac{\mu_r}{2}-1} e^{-x} dx. \quad (6)$$

This completes the specification of the corresponding resonance. The process is terminated once several resonances above the upper URR energy bound have been generated. Extension of the realization beyond the upper bound is needed so that cross sections calculated at an energy just below the bound have the appropriate contribution from resonances existing at both higher and lower energies. The result of neglecting resonances above the upper URR energy bound would be diminished cross section magnitudes just below the crossover to the fast energy region. A similar extension of the resonance generating procedure to energies below the lower URR energy bound is not required as the resolved resonance parameters themselves can be used — albeit in a resonance formalism that may differ from the one that was used in their evaluation — to calculate a contribution to cross section values at the lower end of the URR.

Once a complete realization of resonances — specified by their resonance parameters — is generated over the required energy range for each spin sequence, it can be utilized in a simulation. Procedures presented in [3] can be extended easily enough to

accomplish this as well. Instead of an on-the-fly generation of an energy-localized realization of resonance parameters and direct cross section calculation using those parameters, the same realization of resonance parameters generated at the initialization of a simulation is utilized in all cross section calculations throughout a simulation. Whenever a nuclide’s cross sections must be calculated within a simulation, a number of resonances about the current neutron energy are identified, and their parameters are used to compute the contributions of each of those resonances to the partial cross section values at the desired energy.

Generating new, independent resonance structure realizations for independent transport simulations is as simple as changing the pseudo-random number generator seed used when generating one set of resonances to a different value. Examples of independent realizations of URR resonance structure generated in this manner are shown in Figure 1.

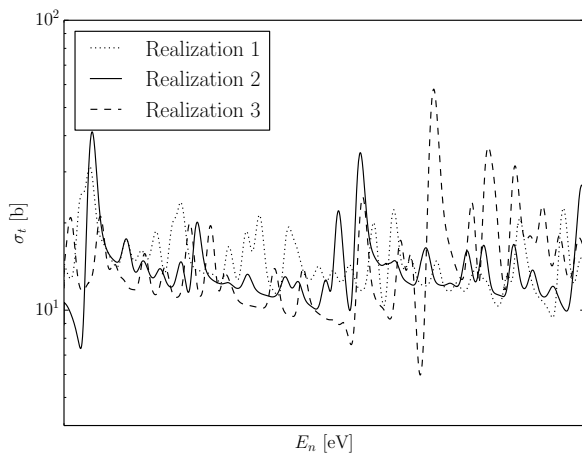


Fig. 1. Independent URR cross section realizations

#### IV. RESULTS AND ANALYSIS

The capability to utilize independent realizations of URR resonance structure is used in simulations of five systems. A light-water reactor (LWR) pin cell is simulated at hot, zero-power (HZP) conditions and the results are presented in Section 1. Results of simulations of a model of the well-known fast spectrum, high-enriched uranium metal sphere Godiva are given in Section 2. Benchmark models of the intermediate/fast spectrum, intermediate-enriched uranium metal split-table assemblies Big Ten and U9 are analyzed in Sections 3. and 4., respectively. Finally, a ZEBRA, core 8H  $k_\infty$  measurement benchmark model is used to obtain the results shown in Section 5.

For each model, 250 independent transport simulations,<sup>1</sup> each using a unique realization of URR resonance structure throughout, are conducted. The expected value  $k$  eigenvalue tallies obtained from each batch of simulations, as well as the statistical spread of those tallies, are examined and compared to the values that are obtained in a single simulation using cross sections computed on-the-fly from a new realization of resonance parameters at each event.

Additionally, each of the five distributions of 250 eigenvalue realizations is tested for normality with both the Shapiro-Wilk [12] and Anderson-Darling [13] tests. The results of these statistical tests are shown in Tables II and III, respectively. The  $p$ -value computed in a Shapiro-Wilk test has the interpretation of being the significance value,  $\alpha$ , at which the null hypothesis of the normality of the sample data can be rejected. The  $A^2$  statistic computed in an Anderson-Darling test has the interpretation of being the critical value above which the null hypothesis of the normality of the sample data can be rejected at the  $\alpha$  corresponding to the critical value. For all distributions, at an  $\alpha$  value of 5%, the null hypothesis that the eigenvalue realizations are drawn from a normal distribution cannot be rejected using either test for normality.

While the apparent normality of the distributions is not required from a theoretical perspective, it is a feature which is helpful when interpreting  $1\sigma$  uncertainties, standard deviations, normal distribution curve fits, etc. To that end, the distribution of eigenvalue realizations for each model is plotted and overlaid with two different normal distributions. One of the distributions is simply a curve fit to the observed data using the sample expected eigenvalue,  $\langle k \rangle$ , and the sample standard deviation of  $k$  realizations,  $SD_k$ . The second curve is the normal distribution that is expected based on statistical uncertainty alone. It is also constructed using  $\langle k \rangle$ , but uses the sample expected value of the standard error of the mean (i.e., the mean of the 250  $1\sigma$  values),  $\langle 1\sigma_k \rangle$ , as its standard deviation. Comparing these two curves enables one to observe the extent to which URR resonance structure uncertainty results in a dispersion of  $k$  realizations. The two principal conclusions which follow from the presented results are that *a single simulation with on-the-fly cross section calculations reproduces the expected value obtained from multiple independent simulations very closely* and *the range of eigenvalues arising from independent URR realizations can be significant*.

##### 1. LWR Pin Cell

First, a pressurized-water reactor pin cell from the Benchmark for Evaluation and Validation of Reactor Simulations [14] is modeled at HZP conditions with the  $UO_2$  fuel, clad, and moderator all at 600 K. Each of 250 independent simulations

<sup>1</sup>This number is selected because it results in relatively tight  $1\sigma$  statistical uncertainties that are also comparable to the  $1\sigma$  values obtained in the simulations with event-based cross section realizations.

TABLE II. Shapiro-Wilk normality test results

Model	$p$ -value
LWR pin cell	0.637
Godiva	0.065
Big Ten	0.347
U9	0.792
ZEBRA	0.331

TABLE III. Anderson-Darling normality test results

Model	$A^2$ (5% Critical Value: 0.775)
LWR pin cell	0.392
Godiva	0.694
Big Ten	0.440
U9	0.297
ZEBRA	0.435

utilizes a different realization of URR resonance structure for  $^{234}\text{U}$ ,  $^{235}\text{U}$ , and  $^{238}\text{U}$ ; 100 discarded source convergence batches; 500 recorded tally batches; and  $1 \times 10^4$  neutron histories per batch. The distribution of  $k_\infty$  eigenvalues computed in these independent simulations is shown in Figure 2, and a summary of the results is given in Table IV.

Figure 2 demonstrates that the observed distribution of  $k_\infty$  realizations is nearly identical to the distribution that is expected as a result of statistical uncertainty alone. This visual agreement is confirmed by the close agreement between the observed sample standard deviation, 0.00044, and the expected sample standard deviation, 0.00041. Table IV also shows very close agreement between the actual expected eigenvalue,  $\langle k_\infty \rangle$ , which is computed by taking the mean of the 250  $k_\infty$  realizations, and the  $k_\infty$  value computed in a single simulation in which new URR resonance structure realizations are generated on-the-fly at each event. Taken together, the preceding observations lead to the somewhat expected conclusion that running multiple simulations of an LWR pin cell with different URR realizations does not provide much information that could not be gleaned in a single simulation with many realizations.

TABLE IV. HZP LWR pin cell results summary

Sample $\langle k_\infty \rangle$	(1 $\sigma$ )	1.35610	(0.00003)
Sample $\text{SD}_{k_\infty}$		0.00044	
Sample $\langle 1\sigma_{k_\infty} \rangle$	(1 $\sigma$ )	0.00041	(<0.00001)
On-the-fly $k_\infty$	(1 $\sigma$ )	1.35618	(0.00004)

## 2. Godiva

Next, 250 independent simulations of the International Criticality Safety Benchmark Evaluation Project (ICSBEP) [15] solid, unreflected sphere model of the Godiva critical assembly (HEU-MET-FAST-001) are performed. Each independent simulation utilizes a different realization of URR resonance structure for  $^{234}\text{U}$ ,  $^{235}\text{U}$ , and  $^{238}\text{U}$ ; 100 discarded source con-

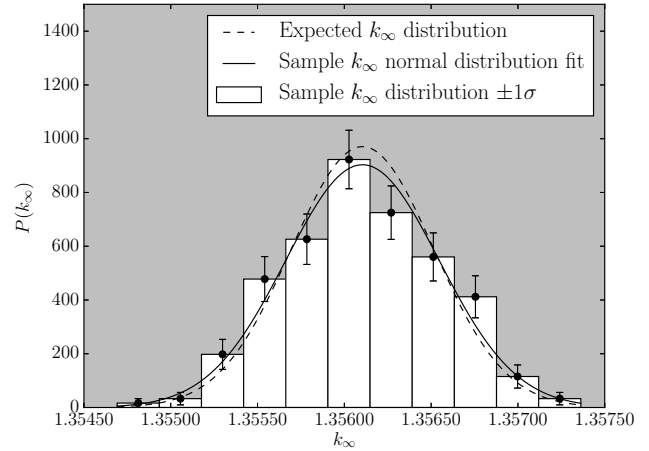


Fig. 2. HZP LWR pin cell  $k_\infty$  PDF for independent realizations

vergence batches; 500 recorded tally batches; and  $1 \times 10^5$  neutron histories per batch.

The distribution of  $k_{\text{eff}}$  eigenvalues is displayed in Figure 3 and a summary of the results is provided in Table V. Much as in the case of the LWR pin cell, Figure 3 illustrates that the actual distribution of  $k_{\text{eff}}$  realizations is quite similar to the distribution that is expected if only statistical uncertainty is considered. The observed sample standard deviation, 0.00012, is relatively close to the expected sample standard deviation, 0.00010. Close agreement is also seen when comparing  $\langle k_{\text{eff}} \rangle$  and the single on-the-fly  $k_{\text{eff}}$  value. Again, averaging multiple independent simulations having different URR realizations produces results similar to an on-the-fly simulation, as is expected considering the peak of Godiva’s exceedingly hard spectrum occurs far above the upper energy bounds of the uranium nuclides’ unresolved regions.

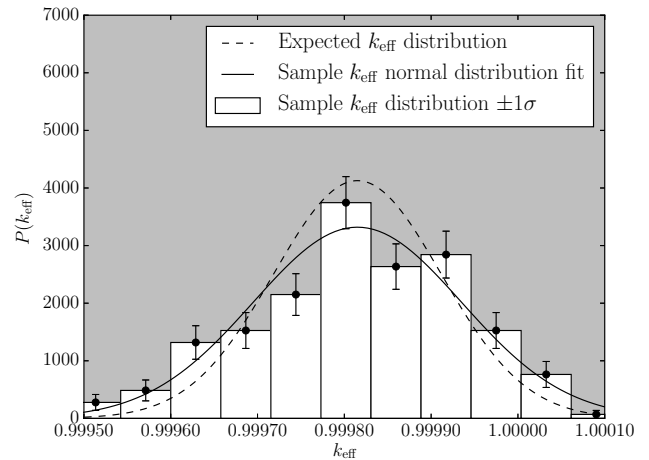


Fig. 3. Godiva  $k_{\text{eff}}$  PDF for independent realizations

TABLE V. Godiva results summary

Sample $\langle k_{\text{eff}} \rangle$	$(1\sigma)$	0.99982	(0.00001)
Sample $SD_{k_{\text{eff}}}$		0.00012	
Sample $\langle 1\sigma_{k_{\text{eff}}} \rangle$	$(1\sigma)$	0.00010	(<0.00001)
On-the-fly $k_{\text{eff}}$	$(1\sigma)$	0.99969	(0.00010)

TABLE VI. Big Ten results summary

Sample $\langle k_{\text{eff}} \rangle$	$(1\sigma)$	1.00533	(0.00003)
Sample $SD_{k_{\text{eff}}}$		0.00055	
Sample $\langle 1\sigma_{k_{\text{eff}}} \rangle$	$(1\sigma)$	0.00010	(<0.00001)
On-the-fly $k_{\text{eff}}$	$(1\sigma)$	1.00530	(0.00006)

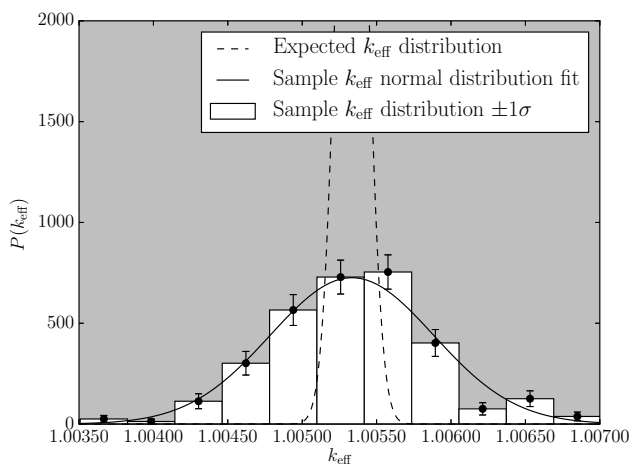


Fig. 4. Big Ten  $k_{\text{eff}}$  PDF for independent realizations

### 3. Big Ten

250 independent simulations of the IEU-MET-FAST-007, case 4 benchmark model of the Big Ten critical assembly from ICSBEP are also performed. Each simulation utilizes a different realization of URR resonance structure for  $^{234}\text{U}$ ,  $^{235}\text{U}$ ,  $^{236}\text{U}$ , and  $^{238}\text{U}$ ; 100 discarded source convergence batches; 500 recorded tally batches; and  $1 \times 10^5$  neutron histories per batch.

The distribution of  $k_{\text{eff}}$  eigenvalues from these simulations is plotted in Figure 4, and a summary of the results is found in Table VI. In contrast to what is observed in the distributions of the LWR pin cell and Godiva eigenvalues, Figure 4 shows that the realized distribution of Big Ten  $k_{\text{eff}}$  values is discernibly broader than the distribution that is generated based on statistical uncertainty alone. The real, observed sample standard deviation is more than five times the expected sample standard deviation. With a normal fit to the  $k_{\text{eff}}$  sample, this leads to an increase in the 95% confidence interval about  $\langle k_{\text{eff}} \rangle$  of more than 150 pcm. It may then be concluded that this discrepancy in standard deviations is attributable to unknown URR resonance structure. However, despite these discrepant uncertainties, close agreement between  $\langle k_{\text{eff}} \rangle$  and the single on-the-fly  $k_{\text{eff}}$  value is observed. So, an on-the-fly simulation and the average of multiple independent simulations having different URR realizations yield comparable eigenvalues, but the uncertainty due to unknown URR resonance structure only reveals itself through multiple independent realizations.

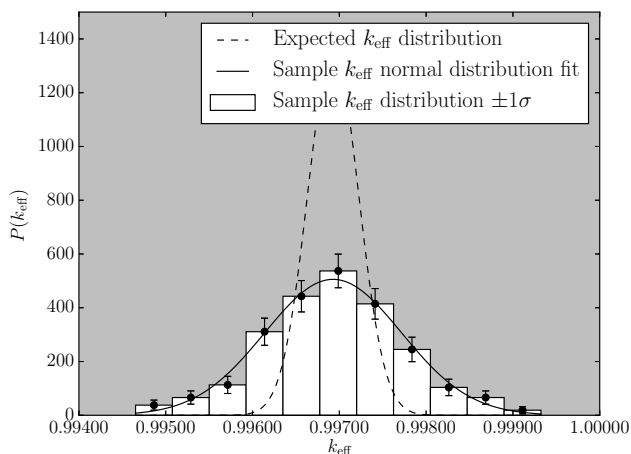


Fig. 5. U9  $k_{\text{eff}}$  PDF for independent realizations

### 4. U9 Benchmark Assembly

The experimental configuration of Assembly 9, Loading 11 at the Zero Power Reactor No. 6 facility (ZPR-6/9) is known as the U9 Benchmark Assembly. The horizontal split-table assembly consisted of a heterogeneous, cylindrical core constructed of alternating enriched and depleted uranium metal plates to give a core-averaged enrichment of 9%. The core was surrounded by a thick depleted uranium reflector resulting in a fast spectrum similar to that of Big Ten. 250 independent simulations of the U9 ICSBEP benchmark model (IEU-MET-FAST-010) are performed. Each simulation utilizes an independent URR resonance structure for  $^{234}\text{U}$ ,  $^{235}\text{U}$ ,  $^{236}\text{U}$ , and  $^{238}\text{U}$ ; 100 discarded source convergence batches; 500 recorded tally batches; and  $1 \times 10^4$  neutron histories per batch.

The distribution of  $k_{\text{eff}}$  eigenvalues and a summary of the results are shown in Figure 5 and Table VII, respectively. As in the case of Big Ten, the distribution of  $k_{\text{eff}}$  highlights the uncertainty in individual eigenvalue realizations due to variability in URR resonance realizations. That is, the distribution of  $k_{\text{eff}}$  values that are actually calculated in simulations relying on different realizations of a single URR resonance structure is significantly broader than the distribution which arises solely from statistical uncertainty. The observed sample standard deviation is nearly three times the expected sample standard deviation leading to an increase in the 95% confidence interval about  $\langle k_{\text{eff}} \rangle$  of more than 200 pcm.

TABLE VII. U9 results summary

Sample $\langle k_{\text{eff}} \rangle$	$(1\sigma)$	0.99693	(0.00005)
Sample $SD_{k_{\text{eff}}}$		0.00079	
Sample $\langle 1\sigma_{k_{\text{eff}}} \rangle$	$(1\sigma)$	0.00029	(<0.00001)
On-the-fly $k_{\text{eff}}$	$(1\sigma)$	0.99692	(0.00010)

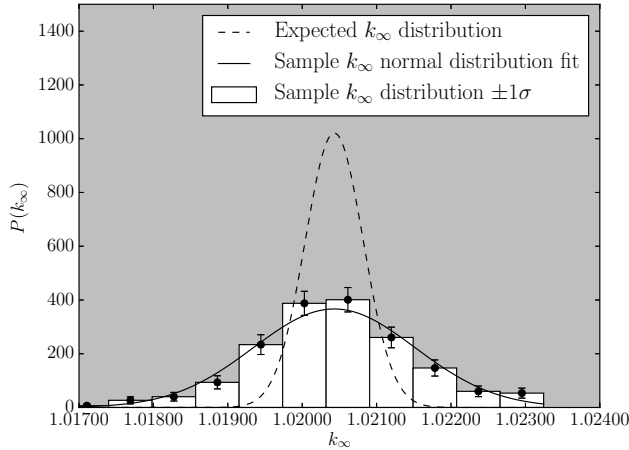


Fig. 6. ZEBRA  $k_{\infty}$  PDF for independent realizations

## 5. ZEBRA

Finally, 250 independent simulations of the Zero Energy Breeder Reactor Assembly (ZEBRA) MIX-MET-FAST-008, core 8H benchmark model from ICSBEP are performed. Each independent simulation utilizes a different realization of URR resonance structure for  $^{235}\text{U}$ , and  $^{238}\text{U}$ ; 100 discarded source convergence batches; 500 recorded tally batches; and  $5 \times 10^3$  neutron histories per batch.

The distribution of  $k_{\infty}$  eigenvalues and a summary of the results are shown in Figure 6 and Table VIII, respectively. To an even greater extent than the cases of Big Ten and U9, the spread of  $k_{\infty}$  illustrates that significant differences in eigenvalue can be observed in simulations with different URR realizations. The sample distribution of  $k_{\infty}$  values calculated in simulations making use of independent realizations of a single URR resonance structure is much broader than the expected distribution due to statistical fluctuations alone. The observed sample standard deviation is more than two times the expected sample standard deviation leading to an increase in the 95% confidence interval about  $\langle k_{\infty} \rangle$  of  $\sim 300$  pcm. What is more, because this additional uncertainty is based on the fundamental lack of knowledge of precise URR resonance structure, it cannot be reduced by simply simulating more neutron histories, nor can it be extracted from a simulation making use of probability tables.

TABLE VIII. ZEBRA results summary

Sample $\langle k_{\infty} \rangle$	$(1\sigma)$	1.02043	(0.00007)
Sample $SD_{k_{\infty}}$		0.00109	
Sample $\langle 1\sigma_{k_{\infty}} \rangle$	$(1\sigma)$	0.00039	(<0.00001)
On-the-fly $k_{\infty}$	$(1\sigma)$	1.02048	(0.00006)

## V. CONCLUSIONS

A capability to construct single, independent URR realizations for use throughout independent continuous-energy Monte Carlo neutron transport simulations is presented. From resonance parameters sampled at the initialization of a simulation, cross sections are calculated on-the-fly. Using this capability, which eliminates the unphysical re-generation of resonance parameters within a simulation, expected value tallies which capture the effect of a persistent URR resonance structure are calculated from multiple independent simulations of models of an LWR pin cell, Godiva, Big Ten, U9, and ZEBRA. Though not a theoretical requirement, these expected values tend to be in good agreement with results calculated with a probability table-like treatment. However, *the spread of eigenvalue realizations coming from simulations using independent URR realizations is much larger than that which is expected based on statistical uncertainty alone. This increased uncertainty is due to the uncertainty in the structure of URR resonances and cannot be decreased by simulating more histories.* Ultimately, this motivates an extension of the most relevant nuclides' (e.g.,  $^{238}\text{U}$ ) resolved resonance region evaluations to higher energies. Additional work should be aimed at applying this capability in simulations of more realistic fast reactor models. Along with this, the effect of URR uncertainties on other parameters of interest, such as Doppler reactivity coefficients, should be investigated.

## VI. ACKNOWLEDGMENTS

This material is based upon work supported by a Department of Energy Nuclear Energy University Programs Graduate Fellowship. This research is supported by the Consortium for Advanced Simulation of Light Water Reactors (CASL), an Energy Innovation Hub for Modeling and Simulation of Nuclear Reactors under U.S. Department of Energy Contract No. DE-AC05-00OR22725. This research is supported by the U.S. Department of Energy (DOE) National Nuclear Security Administration (NNSA) Advanced Simulation and Computing (ASC) program. This work was performed under the auspices of the U.S. Department of Energy by Lawrence Livermore National Laboratory under Contract DE-AC52-07NA27344.

## REFERENCES

1. A. FODERARO, *The Elements of Neutron Interaction*

- Theory*, MIT Press (1971).
2. L. B. LEVITT, “The Probability Table Method for Treating Unresolved Neutron Resonances in Monte Carlo Calculations,” *Nucl. Sci. Eng.*, **49**, 450–457 (1972).
  3. J. A. WALSH, B. FORGET, K. S. SMITH, B. C. KIEDROWSKI, and F. B. BROWN, “Direct, On-the-fly Calculation of Unresolved Resonance Region Cross Sections in Monte Carlo Simulations,” in “Proc. Joint Int. Conf. on Mathematics and Computation (M&C), Supercomputing in Nuclear Applications (SNA) and the Monte Carlo (MC) Method,” (2015).
  4. C. N. KELBER and P. H. KIER, “The Effect of Randomness on Group Cross Sections,” *Nucl. Sci. Eng.*, **24**, 389–393 (1966).
  5. M. W. DYOS, “The Construction of Statistical Neutron Resonances,” *Nucl. Sci. Eng.*, **34**, 181–188 (1968).
  6. A. V. DRALLE, N. R. CANDELORE, and R. C. GAST, “RCPL1- A Program to Prepare Neutron and Photon Cross-Section Libraries for RCP01,” Tech. Rep. WAPD-TM-1268, Bettis Atomic Power Laboratory (1978).
  7. Y. ISHIGURO, S. KATSURAGI, M. NAKAGAWA, and H. TAKANO, “The Construction of Neutron Cross Sections in the Unresolved Resonance Region,” *Nucl. Sci. Eng.*, **40**, 25–37 (1970).
  8. C. R. ADKINS and M. W. DYOS, “The Statistical Uncertainty in Doppler Coefficient Calculations for Fast Reactors,” *Nucl. Sci. Eng.*, **40**, 159–172 (1970).
  9. P. K. ROMANO and B. FORGET, “The OpenMC Monte Carlo Particle Transport Code,” *Ann. Nucl. Energy*, **51**, 274–281 (2013).
  10. E. P. WIGNER, “Results and Theory of Resonance Absorption,” in “Conf. on Neutron Physics by Time-of-Flight,” (1956).
  11. C. E. PORTER and R. G. THOMAS, “Fluctuations of Nuclear Reaction Widths,” *Phys. Rev.*, **104**, 483–491 (1956).
  12. S. S. SHAPIRO and M. B. WILK, “An Analysis of Variance Test for Normality (Complete Samples),” *Biometrika*, pp. 591–611 (1965).
  13. T. W. ANDERSON and D. A. DARLING, “Asymptotic Theory of Certain “Goodness of Fit” Criteria Based on Stochastic Processes,” *Ann. Math. Stat.*, pp. 193–212 (1952).
  14. N. HORELIK, B. HERMAN, B. FORGET, and K. SMITH, “Benchmark for Evaluation and Validation of Reactor Simulations (BEAVRS),” in “Proc. Int. Conf. on Mathematics and Computational Methods Applied to Nuclear Science and Engineering (M&C 2013),” (2013).
  15. “International Handbook of Evaluated Criticality Safety Benchmark Experiments,” Tech. Rep. NEA/NSC/DOC(95)03, NEA Nuclear Science Committee, OECD (2013).